Journal of Thermal Analysis, Vol. 53 (1998) 905-921

THERMOANALYTICAL INVESTIGATION OF SEVERAL LAYERED ZIRCONIUM SALTS AND THEIR DERIVATIVES

Part II

L. Szirtes[1*], *A. M. Szeleczky*[1], *A. O. Rajeh*[1] *and S. K. Shakshooki*[2]

[1]Institute of Isotopes of the Hungarian Academy of Sciences, H-1525 Budapest. P.O.Box 77
Hungary
[2]El-Fateh University Chem. Camp. Tripoli S.P.L.A.J

(Received May 8, 1997)

Abstract

The comparison of data of thermal analysis partly with XRD and/or analytical results permits determination of the exact quantity of crystal water of the investigated samples having quite different behaviour. The compositions of the samples were determined from the results of thermal analysis. Furthermore, the data help elucidate the behaviour of various crystalline materials and also their intercalates during heat treatment.

Keywords: phosphate silica, zirconium

Introduction

The results of thermoanalytical investigations of silica-containing zirconium phosphate, the γ-crystalline form of ZrP are presented in this paper. In the middle of the 1980s new vistas were opened by Alberti and coworkers [1, 2] with the preparation and investigation of an α-layered zirconium salt with two different pendant groups. Some structural and intercalation characteristics of zirconium phosphate-phosphite (ZrPP) have been investigated in our laboratory [3, 4]. The results of thermal analysis of these materials and their intercalates and/or organic derivatives are presented in this paper.

Experimental

Preparation

i – silica-containing α-ZrP was prepared as follows: freshly prepared (via fluoro-complex) α-ZrP was mixed, in the presence of acetate buffer, with

---

* Author to whom all correspondence should be addressed.

1418–2874/98/ $ 5.00

Akadémiai Kiadó, Budapest
Kluwer Academic Publishers, Dordrecht

stoichiometric quantity of sodium metasilicate (Na_2SiO_3) solution at 25±1°C with continuous stirring. The resulting gel was treated with the appropriate quantity of 0.1 mol HCl solution to exchange sodium ions for protons in another experiment Na^+ ions were not exchanged; in this way the sodium salt (with various Na contents) or silica-containing ZrP was obtained. After this, the material was washed with distilled water to pH=4, then heated to 180°C and kept at this temperature for 24 h. The final product was stored in a dessicator over P_2O_5 [5]. Silica-containing ZrPP was synthesized in a similar way with the exception that the final product was stored over saturated NaCl solution [6].

ii – the γ-crystalline form of ZrP (γ-ZrP) was prepared using the method described by Clearfield [7].

iii – zirconium phosphate-phosphite (ZrPP) was prepared in the way proposed by Alberti *et al.* [2], with the exception that various drying methods were used [3].

iiii – the intercalates and/or organic derivatives of the investigated materials were prepared as described earlier by Costantino and also by us [8–15].

The methods used for identification of the prepared samples were described in a paper published earlier [16].

Results and discussion

1. Silica-containing ZrP also has α-layered structure as it was found by XRD analysis, but it has a slightly distorted configuration in comparison with α-ZrP [17, 18]. In Fig. 1 are shown the DTA curves of various samples. As can be seen, the sample (ZrPSi-180) contains the characteristic peaks of both silica and α-ZrP, but at the same time the peaks belonging to the crystalline phase transition are missing from the DTA curves. This phenomenon is in agreement with the XRD data [11] which showed that silica-containing α-ZrP is a one-phase system at the end of preparation. For the Na-containing samples, depending on the amount of wash solution, various $NaPO_4/HPO_4$ ratios were found. By comparison of analytical and weight loss (TG) data, the original materials could be described as:

$$Zr[(HPO_4)_2(SiO_{1.8})_{2.5}OH]\cdot 2H_2O \text{ and}$$

$$Zr[(NaPO_4)_x(HPO_4)_{1-x}(SiO_2)_{2.5}OH]\cdot 2H_2O$$

respectively.

This first endothermic process usually means the loss of crystal water. In the case of silica containing samples this peak is broader due to the relatively small quantity of crystal water and dehydration of silanol OH groups of silica gel occurring at about 170–200°C.

The second endothermic process can be assigned to the loss of structural water, while the exothermic process, without weight loss is connected with the change of crystalline phase of ZrO_2 at about 1000°C [19].

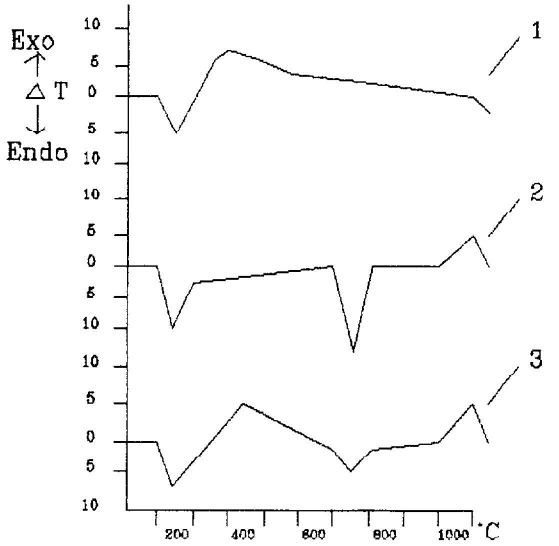

Fig. 1 DTA curves of silica gel(1), α-ZrP(2) and SiZrP(3)

For the sample not treated with HCl solution another exothermic peak was found at about 600°C. In agreement with literature data [20], this process could be identified as the formation of $NaZr_2(PO_4)_3$.

Silica-containing ZrPP showed similar thermal behaviour to that of silica-containing α-ZrP, while silica-containing γ-ZrP was not found at all. From thermoanalytical and XRD data it was concluded that this material is changed into the α-form during the preparation process [6].

2. γ-ZrP also has layered structure but different from α-ZrP, as proved by XRD analysis. Its lattice parameters were found to be a=0.538 nm, b=0.664 nm, c=2.459 nm, and β=94.2° and basal spacing (d)=1.22 nm. Another difference from the α-form was identified by means of IR spectrophotometric method, namely that the phosphate is present in the material in the form of H_2PO_4 and PO_4^{3-} in equal quantities. Thermal analysis provided information about the quantity of crystal water and about the thermal behaviour of this kind of material.

Thermal analysis revealed four endothermic processes (three of them involving mass loss) and one exothermic process. Taking into consideration the results of other analytical methods the first and the third endothermic peaks were identified as the loss of crystal water, while the fourth as the loss of structural water. The endothermic process without mass loss is due to the crystalline phase transition taking place during the loss of part of the crystal water, while the exothermic process is the change of ZrO_2 from cubic to monoclinic form [19].

Analysis of the DTA and TG curves (Fig. 2) reveals that the material contains two moles of crystal water per molecule unit, and these water molecules are bonded in different ways. Taking into consideration the XRD data (measured at elevated temperature) it can be proposed that one mole of crystal water is situated

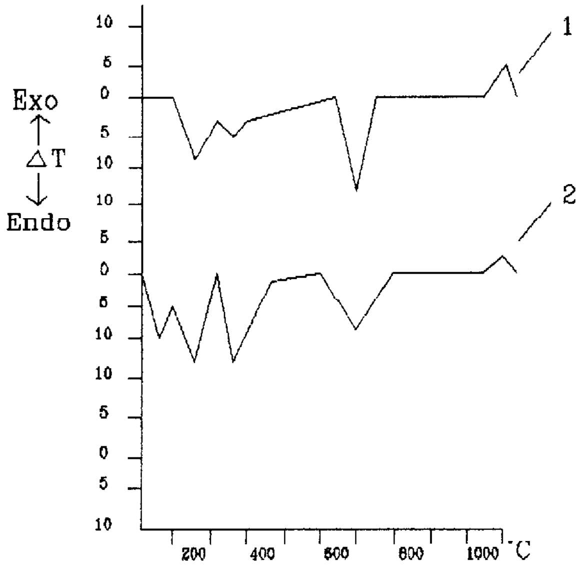

Fig. 2 DTA curves of α-ZrP(1)* and γ-ZrP(2) *prepared via fluoro-complex

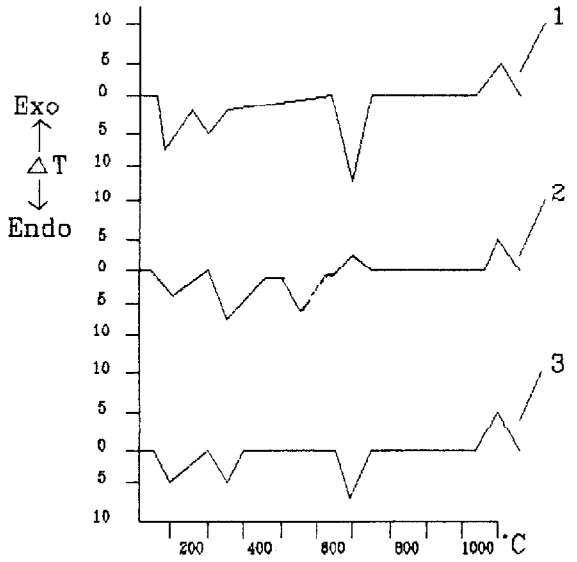

Fig. 3 DTA curve of zirconium phosphate-phosphite (ZrPP) 1-α-ZrP, 2-ZrPP (dried above sat. NaCl sol.), 3-ZrPP (dried under IR lamp on air)

near the metal (Zr) sheets and it is easily lost at a relatively low temperature. As a result of such dehydration, the interlayer distance is decreased from 1.22 nm to 0.95 nm, giving a new crystalline phase as shown by the second endothermic peak in the DTA curve. The second mole of water is lost at a relatively high temperature showing that it had some bonding role between the layeres. The third mole of water lost is the structural water coming from the decomposition of phosphate groups.

Combining the above results with analytical data, the material can be described by the formula $Zr[(H_2PO_4)\cdot(PO_4)]\cdot 2H_2O$ and its thermal decomposition can be characterized as follows:

$$Zr[(H_2PO_4)(PO_4)]2H_2O \xrightarrow[\text{up to }90^\circ C]{-H_2O} Zr[(H_2PO_4)(PO_4)]H_2O \xrightarrow[90-180^\circ C]{\text{phase trans.}}$$

$$Zr[(H_2PO_4)(PO_4)]H_2O \xrightarrow[180-380^\circ C]{-H_2O} Zr[(H_2PO_4)(PO_4)] \xrightarrow[550-620^\circ C]{-H_2O} ZrP_2O_7$$

3. Different modes of drying of the ZrPP resulted different DTA curves of the products, while the total mass loss for both samples was found to be 10%. From the TG curves, taking also the analytical, XRD and IR data into consideration, two different compositions were assumed: one with ‘high’ (dried above saturated NaCl solution) and another with ‘low’ (dried under IR lamp in air) phosphite content. Accordingly, the samples can be described by the chemical formulae $Zr(HPO_4)_{0.7}(HPO_3)_{1.3}\cdot 0.5H_2O$ and $Zr(HPO_4)_{1.8}(HPO_3)_{0.2}\cdot H_2O$, respectively.

The endothermic processes (Fig. 3) in order to characterize the loss of crystal water (up to 130°C), the phase transition (without mass loss) and the loss of structural water. In the case of the sample dried under IR lamp in air practically the same DTA curve was obtained as that of α-ZrP. In accordance with this, the thermal decomposition of the samples may be described as follows:

$$Zr[(HPO_4)_{0.7}(HPO_3)_{1.3}0.5H_2O] \xrightarrow[\text{up to }130^\circ C]{-H_2O} Zr[(HPO_4)_{0.7}(HPO_3)_{1.3}]$$

$$\xrightarrow[140-240^\circ C\ \ 240-340^\circ C]{\text{phase trans. and }-H_2O} Zr[(PO_4)_{0.7}(PO_3)_{1.3}] \xrightarrow[480-540^\circ C]{-0.5H_2O}$$

$$Zr(PO_3)_2 \xrightarrow[610-700^\circ C]{-0.85O_2} ZrP_2O_5$$

For the sample with low phosphite content the thermal decomposition proceeds practically in the same way as in the case of α-ZrP (see in previous paper [16]).

4. Thermal analysis of various intercalates and/or organic derivatives of α-,γ-ZrP, mixed α(Zr,Ti)P and also ZrPP was carried out under the same conditions as described for the original (host) materials. The results of these investigations are collected in Tables 1–4 and shown in Figs 4–9.

Table 1 Composition, total mass loss and interlayer distances of α- and γ-ZrP complexes

Intercaleted molecules	α-ZrP		Composition host/guest mmol/mmol	γ-ZrP		
	interlayer dist. nm	mass loss/ %				
1	2	3	4	2	3	4
MetOH	0.93	39.8	2	1.30	61.1	2
EtOH	1.42	34.6	2	1.54	54.8	2
PropOH	1.66	26.2	2	1.78	44.7	2
BuOH	1.87	26.6	2	2.02	44.8	2.
PenOH	2.13	23.1	2	2.26	43.1	2
MetA	1.28	32.7	1	1.37	52.3	2
EtA	1.47	26.3	1	1.58	46.8	2
PropA	1.69	19.6	1	1.77	42.9	2
BuA	1.88	19.2	1	1.97	42.6	2
PenA	2.09	19.0	1	2.18	42.2	2
D.E.G	1.05	28.8	1.5	1.47	33.4	1.4
Benzyl OH	2.10	41.31	1	2.27	57.26	1
Benzyl A	1.90	22.13	1	2.30	43.11	2
p-nitro benzoic acid	–	–	–	–	–	–
hippuric acid	–	–	–	–	–	–
phenyl phosph. acid	1.47	48.6	0.8	–	–	–

Data for *n*-alkanols are presented in Fig. 4. The α-ZrP-alkanol intercalates (a) lost their crystal water practically together with the alkanol, except the case of ethyl alcohol. In this case the alcohol is lost in a rapid process followed by the loss of crystal water up to 340°C. The next endothermic process with a peak at about 600°C is the loss of structural water, while the exothermic process found between 900–1000°C is connected with the crystalline phase transition of ZrO_2.

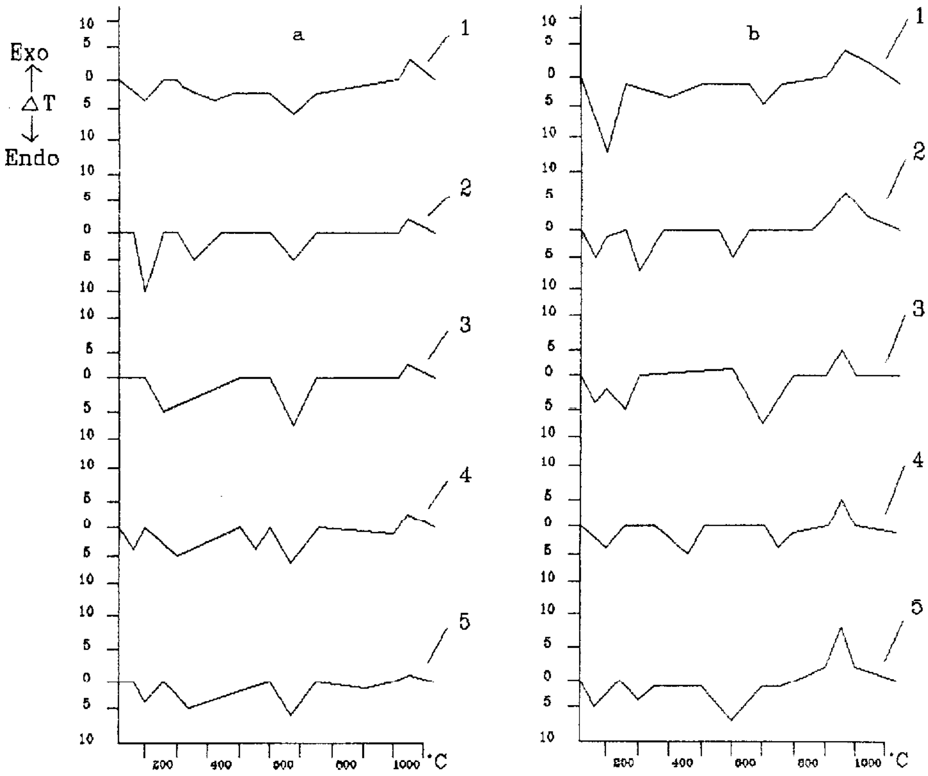

Fig. 4 DTA curves of *n*-alcohol intercalates of α-ZrP(a) and γ-ZrP(b); 1-methyl-, 2-ethyl-, 3-propyl-, 4-butyl-, 5-pentylalcohol

In contrast, for γ-ZrP-*n*-alkanol intercalates (b) these two processes (loss of the alkanol and crystal water) are well separated. The further part of the DTA curves showed no difference from those found for α-ZrP intercalates. The thermal decomposition of these kinds of material can be described, in general, as follows:

i-for α -ZrP

$$\mathrm{Zr[(HPO_4)_2(\mathit{n}\text{-}alkanol)_2]\cdot H_2O} \xrightarrow[\text{up to }430^{\circ}\mathrm{C}]{-2\text{alkanol},\mathrm{H_2O}} \mathrm{Zr(HPO_4)} \xrightarrow{-\mathrm{H_2O}}$$

$$\mathrm{ZrP_2O_7} \xrightarrow[900^{\circ}\mathrm{C}]{} \mathrm{ZrO_2\cdot P_2O_5}$$

ii-for γ-ZrP

$$\mathrm{Zr[(H_2PO_4)(PO_4)(}n\text{-alkanol}\mathrm{)_2]\cdot 2H_2O} \xrightarrow[\text{up to } 110^\circ\mathrm{C}]{-\ 2\ \text{alkanol}} \mathrm{Zr(H_2PO_4)(PO_4)\cdot}$$

$$\mathrm{\cdot 2H_2O} \xrightarrow[110-350^\circ\mathrm{C}]{-2\mathrm{H_2O}} \mathrm{Zr(H_2PO_4)(PO_4)} \xrightarrow[500-650^\circ\mathrm{C}]{-\mathrm{H_2O}} \mathrm{ZrP_2O_7} \xrightarrow[900^\circ\mathrm{C}]{} \mathrm{ZrO_2\cdot P_2O_5}$$

The intercalation behaviour of mixed Zr, Ti phosphates was controlled using ethyl alcohol, *n*-propylamine, *n*-butylamine and ethylenediamine (E.D.A) as guest molecules. The DTA curves or various mixed compounds (complexes) are shown in Fig. 8 (a,b,c).

Table 2 Composition, total mass loss and interlayer distances mixed (Zr, Ti) P-complexes

Host mat.	EtOH	*n*-propyl-amine	*n*-butyl-amine	E.D.A	
$Zr_{0.9}Ti_{0.2}P$	0.84	0.82	0.85	0.86	composition host/guest mmol/mmol
$Zr_{0.5}Ti_{0.5}P$	0.66	0.72	0.56	0.63[a]	
$Zr_{0.2}Ti_{0.3}P$	0.56	0.63	0.56	–	
$Zr_{0.8}Ti_{0.2}P$	21.4	36.3	30.2	33.6[a]	total mass loss / %
$Zr_{0.5}Ti_{0.5}P$	34.5	48.2	39.7	47.5	
$Zr_{0.2}Ti_{0.8}P$	33.7	48.5	33.3	–	
$Zr_{0.8}Ti_{0.2}P$	1.40	1.59	1.84	2.05[a]	interlayer dist. in nm
$Zr_{0.5}Ti_{0.5}P$	1.35	1.55	1.79	1.98	
$Zr_{0.2}Ti_{0.8}P$	1.38	1.57	1.83		

[a] α-ZrP

Thermoanalytical data indicated lower amounts of intercalated EtOH than those found for pure α-ZrP and the amount changed with the Ti content of the sample (0.56 mol/mol ZrP for $Zr_{0.5}Ti_{0.5}$ and 0.84 mol/mol for $Zr_{0.1}Ti_{0.9}$). It was also found that, differing from pure ZrP(EtOH), in this case ethyl alcohol was lost relatively rapidly together with crystal water. At higher temperatures the character of the curves are similar to that of the pure α-ZrP(–EtOH) complex. The thermal decomposition of complexes with various compositions can be described as follows:

$$\mathrm{Zr_xTi_{1-x}(HPO_4)_2(EtOH)_n\cdot}m\,\mathrm{H_2O} \xrightarrow[\text{up to } 180^\circ\mathrm{C}]{-\ n\mathrm{EtOH},\ m\mathrm{H_2O}} \mathrm{Zr_xTi_{1-x}(HPO_4)_2}$$

$$\xrightarrow[370\text{–}600^\circ\mathrm{C}]{-\mathrm{H_2O}} \mathrm{(Zr_xTi_{1-x})P_2O_7}; \quad \text{where } n<1 \text{ and } m=0.5\text{-}1$$

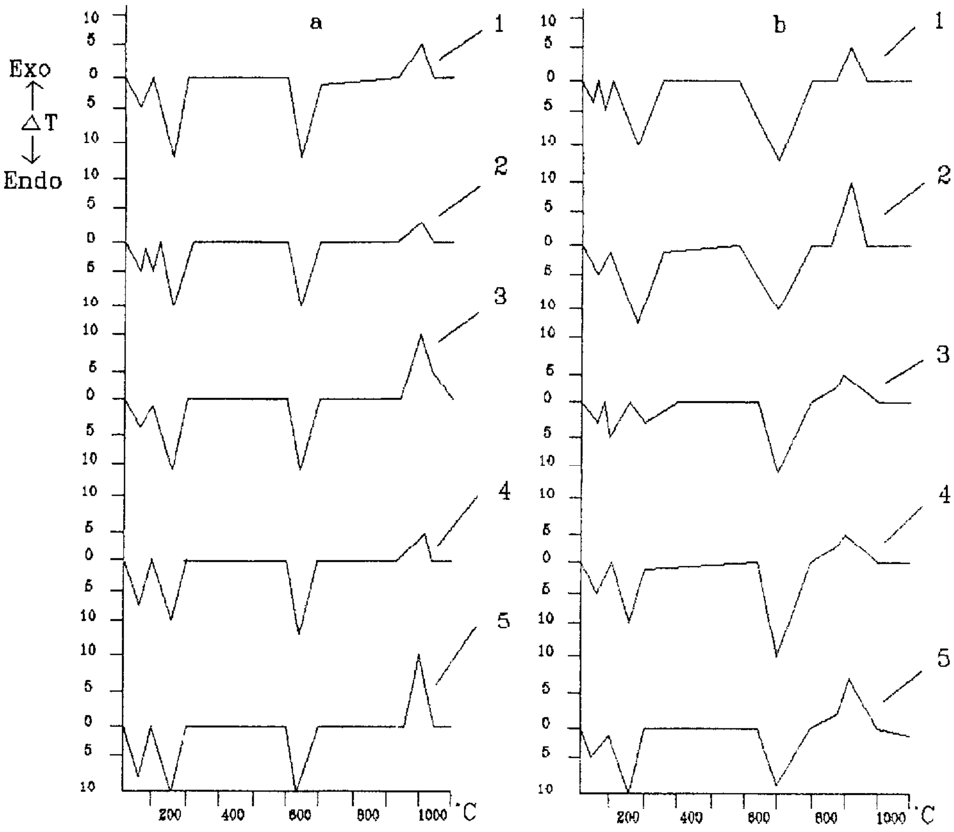

Fig. 5 DTA curves of *n*-monoalkylamine intercalates of α-ZrP(a) and γ-ZrP(b); 1-methyl-, 2-ethyl-, 3-propyl-, 4-butyl-, 5-pentylamine

Data for *n*-monoalkylamines (MAA) are collected in Table 1 and shown in Fig. 5. No characteristic difference appears between the DTA curves of α- and γ-ZrP intercalates. This result was expected since XRD analysis showed that γ-ZrP and α-ZrP had similar structures (see above). In both cases crystal water (one mole/molecule unit) was lost first followed by the decomposition of the monoalkylamine. This was followed by the loss of structural water coming from the decomposition of phosphate groups. For γ-type materials the crystal water was lost in two steps (for C_4 and C_5 amines overlapping with amine decomposition, resulting a running character, without sharp peaks in the DTA curve. On the other hand, the temperature of the third peak was about 50–60°C higher than for the α-complex. The exothermic process near 1000°C is connected with the crystalline phase change of ZrO_2.

Based on the data, the following mechanism of thermal decomposition of MAA intercalates can be proposed:

α-type

$$Zr[(HPO_4)_2{\cdot}MMA]{\cdot}H_2O \xrightarrow[110^{\circ}C]{-H_2O} Zr[(HPO_4)_2{\cdot}MMA]$$

$$\xrightarrow[100-250^{\circ}C]{-MMA} Zr(HPO_4)_2 \xrightarrow[480-600^{\circ}C]{-H_2O} ZrP_2O_7$$

γ-type

$$Zr[(H_2PO_4)(PO_4){\cdot}MMA]{\cdot}2H_2O \xrightarrow[\sim 50^{\circ}C]{-H_2O} Zr[(H_2PO_4)(PO_4){\cdot}MMA]{\cdot}H_2O$$

$$\xrightarrow[\text{up to } 110^{\circ}C]{-H_2O} Zr[(H_2PO_4)(PO_4){\cdot}MMA] \xrightarrow[150-290^{\circ}C]{-MMA} Zr[(H_2PO_4)(PO_4)]$$

$$\xrightarrow[550-680^{\circ}C]{-H_2O} ZrP_2O_7$$

In addition, for *n*-monoalkylamines it was found that the intercalation process has a stepwise character owing to the protonation of MAA and the interaction of ammonium ion with negatively charged species. The heat effects of these processes were determined by means of microcalorimetric method; for *n*-butylamine they are 14.67 kJ mol^{-1} and 1.37 kJ mol^{-1}, respectively [21]. The intercalates of mixed metal phosphates showed different thermal behaviour compared with the MAA complexes of pure ZrP (both α and γ forms, see Table 2). A characteristic difference was found in the release of crystal water. In this case it was lost in several closely following steps. A close correlation was found between this phenomenon and the Ti content of the sample. We assumed that the difference was due to the difference in the structure (in comparison with pure materials) of these complexes.

The structures of the investigated organic derivatives of α- and γ-ZrP are similar (as determined by XRD analysis), the only difference being the location of –P–OH groups which are replaced by –P–OR groups [3, 22]. Since these materials may be regarded as organic-inorganic ion exchangers, it was important to know their thermal behaviour. All the prepared organic derivatives were crystalline with layered structure, having different interlayer distances (Table 1), as shown by XRD analysis.

The DTA curves are shown in Fig. 6. For the benzylalcohol derivative we found three and four endothermic processes with mass loss for α- and γ-ZrP, respectively. They are due to the loss of crystal water (for γ-ZrP in two steps), the decomposition of the organic molecule, and loss of structural water from the de-

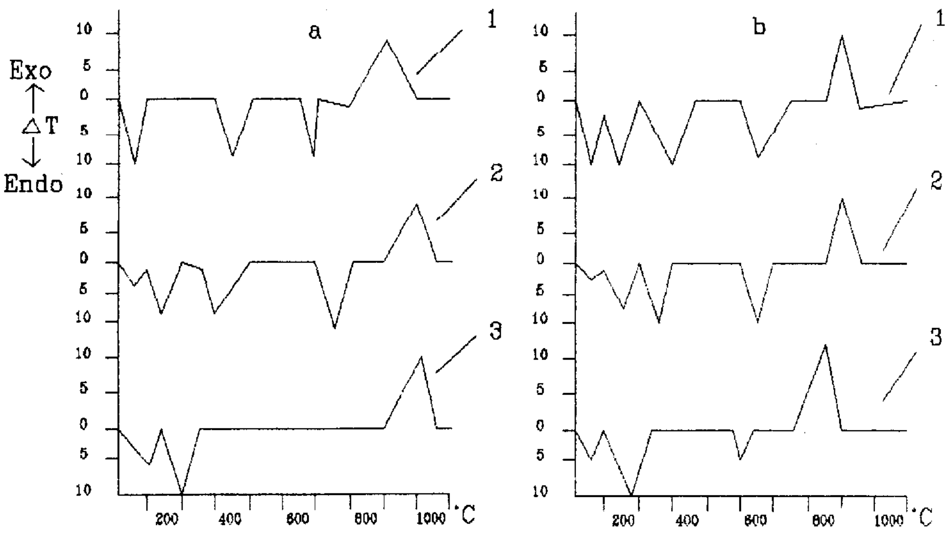

Fig. 6 DTA curves various aromatic intercalates of α-ZrP (a) and γ-ZrP (b). 1 – benzylalcohol, 2 – benzylamine, 3 – diethyleneglycol

composition of phosphate groups. The higher degree of compactness of the γ-form results higher peak temperatures for the mentioned processes.

In the case of benzylamine four endothermic processes were found, of which one occurred without mass loss. The processes can be ascribed to the loss of crystal water and NH_2 group (they are lost together); these processes are finished at about 180°C, and are followed by ring scission. The next process is the decomposition of the organic molecule and at last follows the loss of structural water (for the γ-form at a lower temperature because of the faster decomposition of the $H_2PO_4^-$ groups).

In the case of D.E.G. both the α- and γ-form ZrP derivatives showed similar thermal decomposition character with the exception that γ-[ZrP-D.E.G.] lost its 2 moles of crystal water in one step up to 160°C. This process was followed by the esterification and decomposition of the organic part of the material. At last, up to 600°C decomposed the phosphate groups are decomposed involving release of the structural water which is lost at the same temperature. It must be mentioned that an exothermic process with a peak at 700–750°C without mass loss was observed in all cases. As mentioned earlier, this process can be ascribed to the formation of zirconium pyrophosphate.

The E.D.A. complex of mixed phosphate exhibited similar thermal decomposition as the pure α-ZrP-complex. Namely, they lost their crystal water in a long continuous process, combined with the decomposition of the organic molecule and the loss of amino groups too, followed by the loss of structural water (peak at about 550°C).

The character of the DTA curve changed with increasing Ti content: the crystal water was lost in a more distinct process with a peak at about 100°C and it was followed by the destruction of the organic molecule accompanied by an endothermic peak at about 360°C. The thermal decomposition can be characterized as follows:

a/ sample with lower Ti content

$$[Zr_{0.66}Ti_{0.33}(HPO_4)_2 0.86EDA]\cdot H_2O \xrightarrow[\text{up to } 450^{\circ}C]{(-H_2O + EDA)} Zr_{0.66}Ti_{0.33}(HPO_4)$$

$$\xrightarrow[450\text{–}550^{\circ}C]{-H_2O} (Zr_{0.66}Ti_{0.33})P_2O_7$$

b/ sample with lower Zr content

$$[Zr_{0.33}Ti_{0.66}(HPO_4)_2 0.86EDA]\cdot H_2O \xrightarrow[\text{up to } 120^{\circ}C]{-H_2O} Zr_{0.33}Ti_{0.66}(HPO_4)_2 0.86$$

$$\xrightarrow[150\text{–}450^{\circ}C]{-\ 0.86EDA} Zr_{0.33}Ti_{0.66}(HPO_4)_2 \xrightarrow[450\text{–}550^{\circ}C]{-H_2O} (Zr_{0.33}Ti_{0.66})P_2O_7$$

The amount of crystal water was determined from TA data (for the samples one mole was found per molecule unit). It was also found that the thermal decomposition in both cases was finished by the formation of the pyrophosphate of mixed metals.

Aromatic compounds (benzylalcohol, benzylamine, benzoic acid, hippuric acid, and phenylphosphonic acid) as intercalates of α- and γ-ZrP and ZrPP were also investigated. It was found that the α-ZrP intercalates are similar to the aniline derivatives, but the interlayer distances of the final products are different, depending on the route of intercalation (Table 1).

Table 3 Composition, total mass loss and interlayer distance of intercalation complexes

Host material	Benzyl alcohol	Benzyl amine	Hippuric acid	
α-$Zr(HPO_4)_2\cdot H_2O$ [α-ZrP]	0.2[a] 2[b]	0.2[a] 2[b]	0.1[a] 0.8[b]	composition hist/guest mmole/mmole
	27.3[a] 23.4[b]	27.3[a] 23.4[b]	27.1[a] 25.6[b]	total mass loss/%
	0.99[a] 1.00[b]	0.98[a] 1.87[b]	1.01[a] 1.85[b]	interlayer dist./ nm

[a] preparation via α-ZrPEtOH complex

[b] preparation via back titration of 4-propylamine complex of α-ZrP

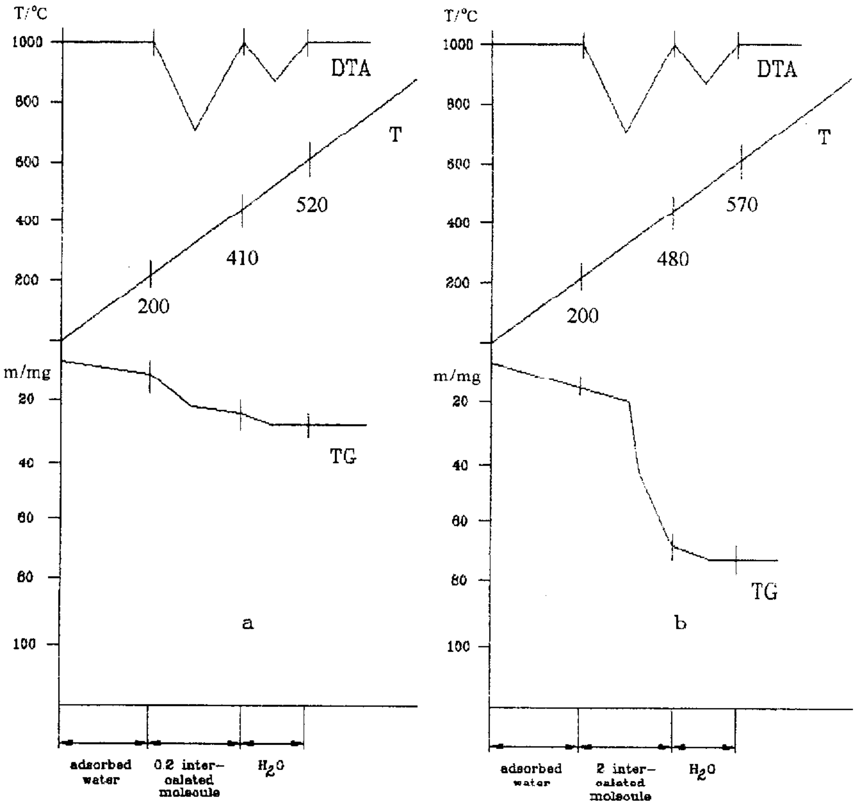

Fig. 7 Typical DTA and TG curves of various intercalates of ZrP type matrix. a – Bronsted-base type molecules, b – Weak-base molecules

Table 4 Composition, total mass loss and interlayer distance of ZrPP-intercalated complexes

Host material	Benzyl alcohol	Benzyl amine	*p*-nitro-benzoic acid	Hippuric acid	Phenyl-phosphonic acid	
	1^b 1^c	0.3^b 2^c	0.4^b 1^c	0.3^b 1^c	0.5^b 1^c	composition host/guest mmol/mmol
α-Zr$(HPO_4)_{0.7}(HPO_3)_{1.3}\cdot 0.5H_2O$ [α-ZrPP]	54.3	47.7	42.1	34.4	62.6	total mass loss / %
	2.42^b 1.73^c	– 1.70^c	– 1.76^c	1.01^a 1.69^c	– 1.81^c	interlayer dist. / nm

[b] preparation via back titration of 4-propylamine complex of α-ZrP
[c] directly reacted from conc. solution

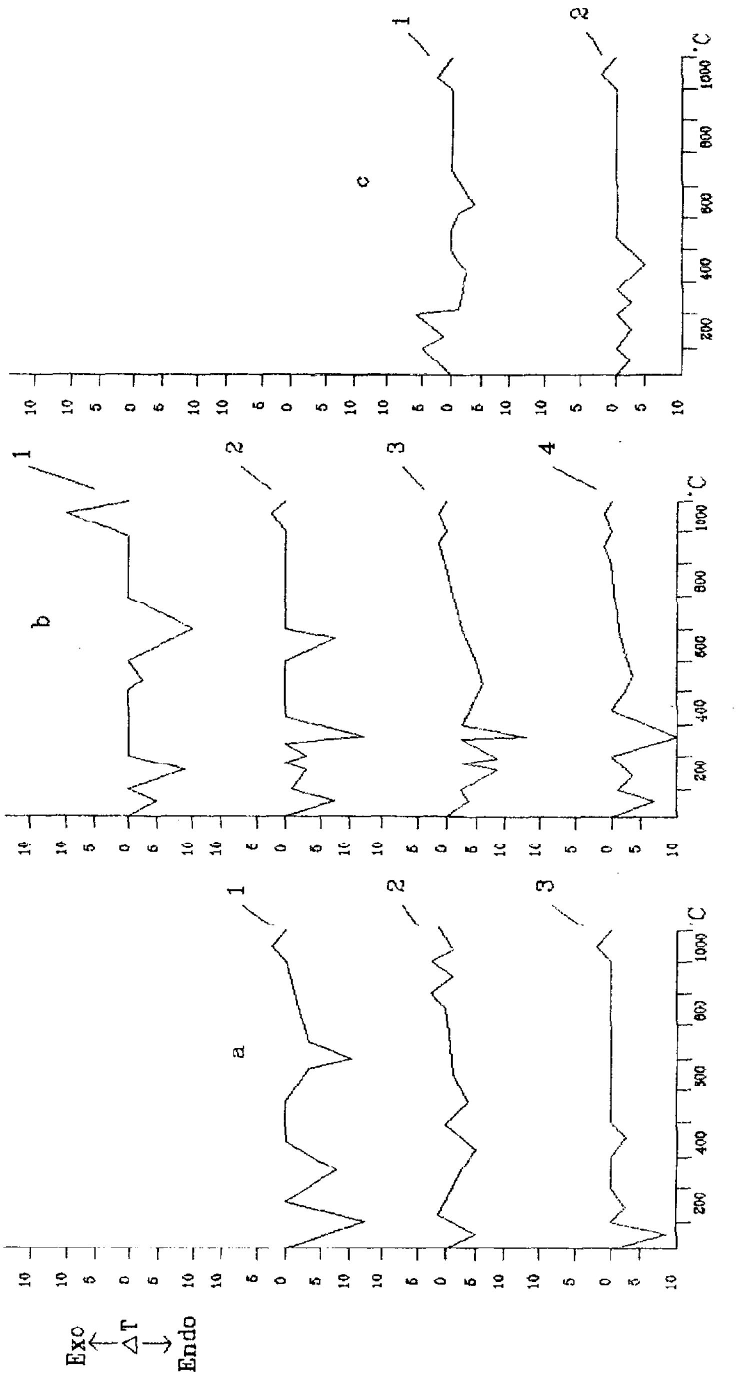

Fig. 8 DTA curves of various intercalates of mixed Zr, Ti phosphates (ZrTiP)

a - ethylalcohol
1-α-$Zr_{0.8}Ti_{0.2}P$
2-α-$Zr_{0.5}Ti_{0.5}P$
3-α-$Zr_{0.2}Ti_{0.8}P$

b - *n*-butylamin
1-α-$Zr_{0.8}Ti_{0.2}P$
2-α-$Zr_{0.5}Ti_{0.5}P$
3-α-$Zr_{0.2}Ti_{0.8}P$

c - E.D.A
1-α-ZrP(EDA)
2-α-$Zr_{0.5}Ti_{0.5}P$(E.D.A.)

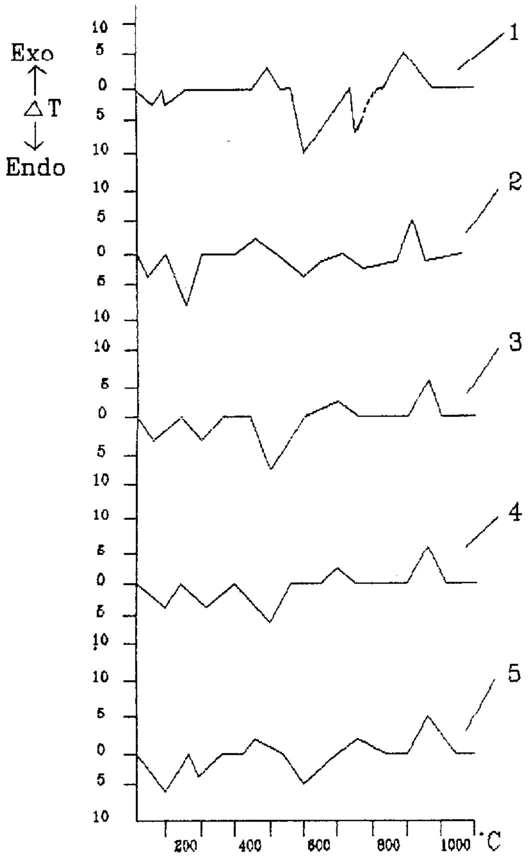

Fig. 9 DTA curves of aromatic intercalates of ZrPP. 1 – benzylalcohol, 2 – benzylamine, 3 – hippuric acid, 4 – *p*-nitrobenzoic acid, 5 – phenylphosphonic acid

When the preparation went through the [ZrP·(EtOH)$_2$] complex the interlayer distance of the product was referred to an arrangement in which the aromatic rings are oriented parallel to the zirconium planes of ZrP, forming monolayers of intercalated molecules [14]. The same situation was observed for γ-ZrP, too [23]. The composition of intercalated complexes was determined partly by thermal analysis. Data are collected in Table 3. The host/guest ratio was found to be 0.1–0.2 mole of intercalated aromatics per mole of ZrP.

In the case of preparation via the [ZrP(*n*-propylamine)] complex, both the interlayer distance and the host/guest ratio (it was found 2) were found near that of the aniline intercalation complex; this fact suggested that the intercalated organic molecules have formed a double layer between the planes of ZrP. In Fig. 7 typical DTA and TG curves of the named intercalates are shown. The curves have typical character, namely they show the loss of crystal water, the decomposition of organic substance and the loss of structural water. At the same time, the DTA curves are not so clear as they were in case of the above discussed materials, because of the continuous evaporation of adsorbed solvent.

Using the so called contact method (contacting a saturated solution of the organic molecule with ZrP for 4 –6 days at 40°C) similar results were obtained as in the case of the previous method.

Zirconium phosphate-phosphite (ZrPP) has a structure different from those of α- and/or γ-ZrP, thus it was interesting to known whether or not it is capable of intercalating organic molecules and to find a method of intercalation. The DTA curves of the organic molecules containing COOH and/or NH_2 groups used are presented in Fig. 9. The organic/inorganic molecular ratios are collected in Table 3.

In the case of benzylamine and phenylphosphonic acid a ratio of 2 was found. Of the four endothermic processes – found for the benzylalcohol intercalate – two are connected with the loss of crystal water and alcohol (the amount of crystal water was determined as 0.5 mole/molecular unit for all the investigated samples), the third with the destruction of the benzyl ring, and the fourth with the loss of structural water. The DTA curve of benzylamine intercalate has the same character with peaks at the same temperature.

In the case of hippuric acid the DTA curve showed endothermic peaks involving weight loss at 80, 200, 405 and 700°C and also exothermic processes with peaks at 500 and 900°C without weight loss. The first two endothermic processes are due to the loss of crystal water and amino groups, respectively. The third is connected with the liberation of the acid ring, and the fourth to the loss of structural water. Of the exothermic processes the first is due to the destruction of the organic molecule.

Practically the same character was found for the DTA curve of the *p*-nitrobenzoic acid complex, with the difference that the third endothermic and the first exothermic peaks are due to ring scission and total decomposition of the organic molecule.

In the case of the phenylphosphonic acid derivative three endothermic peaks involving weight loss (80, 510, 700°C) and two exothermic peak without mass loss (440, 900 °C) were found. The first endothermic process is the loss of crystal water, the second – together with the first exothermic process – the decomposition of the phenyl ring while the third the loss of structural water. The second exothermic process, in all cases, is the formation of pyrophosphate.

Comparison of these data with those of α-ZrP reveals two main differences:

i) – the latter complexes are more stable *vs.* heat (the analogous peaks are observed at higher temperature);

ii) – based on the compilation of thermal and XRD data it was possible to determine that the intercalation went into the phosphate layers [15]. It must be noted that ZrPP can intercalate organic molecules more easily than α-ZrP to an extent that even acidic species have been directly intercalated.

The present investigations provided a comprehensive picture about the thermal behaviour of the materials studied and in many cases the results of thermal analysis help elucidate the structure of these complexes and also the mechanism of intercalation processes.

Conclusions

The comparison of data of thermal analysis with XRD and/or analytical chemistry results permits determination of the exact quantity of crystal water in the investigated samples with different characters. Beside this, based on the results of thermal analysis the compositions of the samples were given. Furthermore, the data make clear the behaviour of various crystalline materials and also their intercalates during heat treatment. It became clear that in all cases the crystal water was first lost as a result of which a new crystalline phase was formed; it was found that the α- and γ-crystalline forms of ZrP had different (well distinguished) behaviour during heat treatment. In all cases, the structural water was lost at last (in the interval 500–700°C) which came from the decomposition of phosphate groups. Based on these results a complete picture was obtained about the way of thermal decomposition of the investigated samples representing a wide variety of crystalline zirconium phosphate compounds.

References

1 G. Alberti, U. Costantino and G. Perego, J. Solid State Chem., 63 (1986) 455.
2 G. Alberti, U. Costantino, F. Marmottini and G. Perego, React. Polym., 9 (1988) 267.
3 A. O. Rajeh, Thesis for Ph. D. Inst. of Isot., Budapest, 1990.
4 L. Szirtes and A. O. Rajeh, J. Radioanal. Nucl. Chem., Art., 196 (1995) 311.
5 Le Van So and L. Szirtes, J. Radioanal. Nucl. Chem., Art., 99 (1986) 45.
6 L. Szirtes, unpublished data.
7 A. Clearfield, R. H. Blessing and J. A. Stynes, J. Inorg. Nucl. Chem., 30 (1968) 2249.
8 G. Alberti and U. Costantino, in Intercalation Chemistry M. S. Whittingham, A. A. J. Jacobson (eds) Academic Press, Paris 1982. Chap. 5.
9 U. Costantino, J. Inorg. Nucl. Chem., 43 (1981) 1985.
10 S. Yamanaka and T. Tanaka, J. Inorg. Nucl. Chem., 41 (1979) 45.
11 L. Szirtes, J. Környei and Z. Pokó, J. Radioanal. Nucl. Chem. Art., 81 (1984) 291.
12 J. Környei and L. Szirtes, ibid, 83 (1984) 521.
13 J. Környei, L. Szirtes and U. Constantino, ibid., 89 (1985) 331.
14 L. Szirtes, J. Környei and Z. Pokó, React. Polym., 7 (1988) 185.
15 L. Szirtes and A. O. Rajeh, Solid State Ionics, 46 (1991) 69.
16 L. Szirtes, S. K. Shakshooki, A. M. Szeleczky and A. O. Rajeh, J. Therm. Anal. Cal., 51 (1998) 503.
17 L. Szirtes, Solid State Ionics, 61 (1993) 145.
18 L. Szirtes and E. Kuzmann, J. Radioanal. Nucl. Chem. Lett., 200 (1995) 159.
19 W. B. Blumenthal, The Chemical Behaviour of Zirconium van Nostrand, Princeton 1958.
20 A. La Ginestra and M. A. Massucci, Thermochim. Acta, 32 (1979) 241.
21 I. Dékány and L. Szirtes, J. Radioanal. Nucl. Chem. Art., 190 (1995) 167.
22 G. Alberti and U. Costantino, J. Molecul. Catal., 27 (1984) 237.
23 L. Szirtes, Thesis for D. Sci. Hung. Acad. Sci. Budapest, 1987.